



Proteomic analysis of male zebrafish livers chronically exposed to perfluorononanoic acid

Wei Zhang^{a,b,1}, Yang Liu^{a,1}, Hongxia Zhang^a, Jiayin Dai^{a,*}

^a Key Laboratory of Animal Ecology and Conservation Biology, Institute of Zoology, Chinese Academy of Sciences, Beijing, 100101, PR China

^b Graduate School of the Chinese Academy of Sciences, Beijing 100080, PR China

ARTICLE INFO

Available online 9 April 2011

Keywords:

Perfluorononanoic acid
Proteomics
2-D DIGE
Hepatotoxicity
PPAR
Male zebrafish

ABSTRACT

Perfluorononanoic acid (PFNA), a synthetic perfluorinated carboxylic acid and fluorosurfactant, is a known environmental contaminant found in people and wildlife. To understand the hepatotoxicity mechanism of PFNA, male zebrafish ($n = 200$) were exposed to differing concentrations of PFNA (0, 0.1, 0.5, and 1.0 mg/L) for 180 days. A two-dimensional difference gel electrophoresis (2-D DIGE) approach coupled with MALDI-TOF-MS/MS analysis was employed to detect and identify the differential expressed proteins. A total of 57 proteins were successfully identified and categorized into functional classes that included metabolism (amino acid metabolism, TCA cycle and pyruvate metabolism, gluconeogenesis and glycolysis, protein metabolism and modification, and nucleotides metabolism), structure and motility, stress and defense, signal transduction, and cell communication. Our proteomic analyses added new perspective to PFNA hepatotoxicity in zebrafish. Results regarding mRNA levels demonstrated that the involvement of peroxisome proliferator-activated receptors (PPARs) could not sufficiently explain the hepatotoxicity mechanism of PFAAs in zebrafish. The extensive protein variations indicated that multiple cellular pathways were involved in and suggested that multiple protein molecules should be simultaneously targeted as an effective strategy to counter PFNA toxicity. Other potential modes should be further investigated.

© 2011 Elsevier Ltd. All rights reserved.

1. Introduction

Perfluorinated alkyl acids (PFAAs), which consist of a carbon backbone with hydrogen replaced by fluorine (Dinglasan-Panlilio and Mabury, 2006), are highly resistant to degradation and have been widely used as surfactants in a variety of products (Renner, 2001). As a result, these chemicals and their potential precursors have been found worldwide (Karrman et al., 2007; Lau et al., 2007; Tao et al., 2008) and scientific and regulatory concerns about potential health risks to humans and wildlife have grown due to their global distribution (Lau et al., 2007). Consequently, manufacturing emissions of PFAAs such as perfluorooctanesulfonate (PFOS) and perfluorooctanoate (PFOA) have decreased (Lau et al., 2007). However, longer alkyl chains of PFAAs remain unregulated (Jensen and Leffers, 2008) and chemicals such as perfluorononanoic acid (PFNA), a nine carbon backbone of PFAAs, continue to increase worldwide. For example, perfluorinated chemicals have been measured in very high concentrations in Russian Baikal seals (*Phoca sibirica*) (Ishibashi et al., 2008), bottlenose dolphins (*Tursiops truncatus*) from Delaware Bay (Houde et al., 2005), and polar bears (*Ursus maritimus*) (Smithwick et al., 2005). Significantly, PFNA has also been detected in human seminal plasma (Guruge et al., 2005) and milk

(Karrman et al., 2007; So et al., 2006). In addition, some precursors such as fluorotelomer alcohols may be transformed into PFNA during the environmental degradation processes, which increases the bio-availability of this chemical to living organisms. In a cross-sectional study between 1999–2000 and 2003–2004, for example, mean concentrations of PFNA increased two-fold in the US population's blood serum (Calafat et al., 2007). This increase has also been seen in wildlife species, such as the ten-fold increase in PFNA levels seen in northern sea otters (*Enhydra lutris*) from 2004 to 2007 (Hart et al., 2009).

Previous studies have shown that PFAAs, such as PFOA and PFOS, induce immune toxicity (Yang et al., 2001), neuron toxicity (Lau et al., 2007), and reproductive and developmental toxicity in rodents (Lau et al., 2004), and have even induced liver, testicular, pancreatic and breast cancer (Hekster et al., 2003). Most studies have demonstrated that the effects of PFAAs on the liver, including increased liver-to-body weight ratios, hepatocellular hypertrophy, vacuolation (Seacat et al., 2003), peroxisome proliferation, and changes in lipid metabolism (Kennedy et al., 2004), were initiated by the activation of peroxisome proliferator-activated receptors (PPARs) in rodents. Recently, several studies have demonstrated that PFAAs activate PPAR isoforms and their target genes (Takacs and Abbott, 2007; Vanden Heuvel et al., 2006). In addition, the activity and expression of several hepatic enzymes involved in fatty acid metabolism and cholesterol synthesis were altered following low-dose PFAAs treatments (Guruge et al., 2006).

* Corresponding author. Tel.: +86 10 64807185; fax: +86 10 64807099.

E-mail address: daijy@ioz.ac.cn (J. Dai).

¹ These authors contributed to this work equally.

Unlike rodents, however, only limited research has examined the toxic mechanisms of PFAAs in teleostean livers. In vivo hepatotoxicity studies have demonstrated that PFOS interferes with DNA metabolism homeostasis and induces inflammation-independent enzyme leakage in common carp (*Cyprinus carpio*) (Hoff et al., 2003), influences membrane permeability of hepatocytes in gibel carp (*Carassius auratus gibelio*), common carp, and eel (*Anguilla anguilla*) (Hoff et al., 2005), and increases fatty acyl-CoA oxidase activity and induces oxidative stress in fathead minnow (*Pimephales promelas*) and rainbow trout (*Oncorhynchus mykiss*) (Oakes et al., 2004; Oakes et al., 2005). In vitro, exposure to PFOS and PFOA for 24 h produced oxidative stress and induced apoptosis in primary cultured hepatocytes of freshwater tilapia (*Oreochromis niloticus*) (Liu et al., 2007). In our previous study, alterations in gene expression associated with lipid metabolism and transportation, hormone action, immune responses, and mitochondrial function were observed in rare minnow (*Gobiocypris rarus*) livers after PFOA exposure (Wei et al., 2008) and oxidative stress was observed in zebrafish (*Danio rerio*) livers after exposure to perfluorododecanoic acid (PFDoA) (Liu et al., 2008). The hepatotoxicity mechanisms of individual perfluoroalkylated substances are, however, not well understood. Thus, global functional analyses are warranted to explore the complicated biochemical mechanism of PFAAs in teleosts.

Proteomics is a powerful method that provides insight into the mechanisms of toxic compounds (Wetmore and Merrick, 2004). Specifically, proteome analysis provides an effective way to identify new proteins and discover the complex effects of toxic chemicals and related biomarkers for risk assessment (Kleno et al., 2004; Shi et al., 2009; Wei et al., 2008). In the present study, a two-dimensional difference gel electrophoresis (2-D DIGE) approach was employed to examine alterations in protein expression in zebrafish livers following chronic exposure to PFNA. Several relevant gene expression changes were measured to clarify the underlying mechanisms of PFNA toxicity. In addition, mRNA levels of PPARs and their downstream target genes involved in lipid homeostasis were investigated by quantitative real-time PCR (qRT-PCR). Based on proteomic analysis and transcriptional data, this work will help clarify the underlying mechanisms of chronic PFNA toxicity and evaluate the potential long-term ecological risks of perfluorinated chemicals.

2. Materials and methods

2.1. Materials

The PFNA was obtained from Sigma Aldrich (CAS number 375-95-1, 97% purity). Solvent-free stock solutions of PFNA were prepared by dissolving crystals in water with stirring. Two stock solutions of 10 and 100 mg/L were used to span the desired range of target solution in exposure water.

2.2. Animals and treatment

The same brook male offspring ($n=200$) from eight pairs of breeding zebrafish (wild-type, *Tuebingen* strain) were provided by Peking University zebrafish resource. They were kept in aerated fresh water tanks and fed three times a day. Fry 5–12 days past fertilization (dpf) were fed paramecia, 12–20 dpf were fed live brine shrimp (*Artemia salina*) and paramecia, and from 21 dpf onwards were fed with live brine shrimp. The PFNA exposure was initiated once the zebrafish developed to 23 dpf and it lasted for a total of 180 days. Using a static-renewal procedure, juveniles ($n=200$) were randomly assigned to nominal concentrations of 0 (control), 0.1, 0.5, and 1.0 mg/L of PFNA. All fish were held under the same photoperiodic regime of 16-h light:8-h dark, and water quality parameters of 24–26 °C and 8.1–8.3 pH. After 180 days exposure, all fish were

anesthetized on ice for sampling. Their livers were surgically removed after blood was taken from the tail fin using a glass capillary; one part was placed in Bouin's fixative and the rest immediately frozen in liquid nitrogen and stored at -80 °C until analysis.

2.3. Histopathological analysis

Liver tissues fixed in 10% formalin were processed sequentially in ethanol, xylene, and paraffin. Tissues were then embedded in paraffin wax, sectioned (4–5 μ m), and mounted on slides. The sections were subsequently stained with haematoxylin and eosin.

2.4. Protein preparation

Total protein of the frozen fish liver was extracted using TRIZOL reagent (Invitrogen Corp., Carlsbad, CA) according to the manufacturer's instructions and was redissolved in lysis buffer (7 M urea, 2 M Thiourea, 4% (w/v) CHAPS, 30 mM Tris, 1 mM PMSF and 1% protease inhibitor cocktail (Sigma-Aldrich, St. Louis, MO)). Protein concentration was determined by 2-D Quant protein assay kit (GE Healthcare, Uppsala, Sweden). Equal amounts of protein sample from two random individual fish in the same treatment group were pooled. Each group yielded three pooled protein samples, and the pH values of the samples were adjusted to 8.5 with 100 mM of sodium hydroxide before labeling. Approximately 50 μ g of protein from all treatment and control groups was then labeled with 400 pmol CyDye Fluor minimal dyes (GE Healthcare) of either Cy3, Cy5, or Cy2 (Cy2 was used to label internal standard (IS)) as described in the manufacturer's protocols. Samples labeled with different dyes (Table S1 (Supplementary data)) were combined and mixed with 450 μ L of rehydration buffer (7 M urea, 2 M Thiourea, 2% CHAPS, 0.5% IPG buffer 4–7, 20 mM DTT and a trace of bromophenol blue) prior to isoelectric focusing (IEF) and subsequent SDS-PAGE.

2.5. 2-D DIGE and image analysis

The labeled mixtures were loaded onto immobiline dry strips (24 cm, linear pH gradient from pH 4–7, GE Healthcare). Isoelectric focusing was conducted for a total of 78 kVh on a Multiphor II system (GE Healthcare) after rehydrating the IPG strips at 40 V for 5 h followed by 100 V for 6 h. The strips were equilibrated and then applied to 12.5% polyacrylamide gels after the IEF program was completed. SDS-PAGE was performed using the Ettan™ Dalt Six Equipment (GE Healthcare) at 15 °C. All electrophoresis procedures were performed in the dark. Silver staining was performed after the gels were scanned using a Typhoon™ Trio Series Variable Mode Image (GE Healthcare) at 100 μ m resolution. The resulting gel images were analyzed using DeCyder software 6.5 (GE Healthcare). The differential in-gel analysis (DIA) mode was used to co-detect spots from four images of a gel (internal standard and three samples) and normalize the spot volume ratios of the Cy3- and Cy5-labeled spots with reference to the Cy2-labeled internal standard from the same gels. The biological variation analysis mode (BVA) then allowed inter-gel matching on the basis of IS (Cy2) and revealed differences between PFNA-treated groups and the control group across all gels. A Student's t-test was used to statistically analyze the data, and $p<0.05$ was considered significant.

2.6. In-gel digestion and MALDI TOF/TOF analysis

Protein spots, altered expression levels between the control and treatment groups, were excised manually from silver-stained gels and subjected to in-gel trypsin digestion. Briefly, gel pieces were de-stained for 20 min at room temperature using 15 mM of potassium ferricyanide and 50 mM of sodium thiosulfate (1:1). Gels were then

washed twice with deionized water and shrunk by dehydration in acetonitrile (ACN). The samples were then rehydrated in a digestion buffer (20 mM ammonium bicarbonate, 12.5 ng/μL trypsin) at 4 °C. After 30 min of incubation, the gels were digested for more than 12 h at 37 °C. Peptides were then extracted twice using 0.1% TFA in 50% ACN. The extracts were dried and eluted onto the target with 0.7 μL of matrix solution (α-cyano-4-hydroxy-cinnamic acid in 0.1% TFA, 50% ACN). Samples were allowed to air-dry before being analyzed by an ABI 4700 MALDI-TOF/TOF Proteomics Analyzer (Applied Biosystems, Framingham, MA, USA). Positive ion mass spectra were recorded on a home-built linear time-of-flight mass spectrometer using 39 kV of total acceleration energy. Data from the peptide mass fingerprint (PMF) and MALDI-TOF MS/MS were analyzed using MASCOT (Matrix Science, London, UK) search software. The following parameters were used in the search: *Danio rerio*, protein molecular mass ranged from 700 to 3000 Da, trypsin digest with one missed cleavage, peptide tolerance of 0.2, MS/MS tolerance of 0.8 Da, and possible oxidation of methionine. Based on the combined MS and MS/MS spectra, protein scores greater than 58 were considered statistically significant ($p < 0.05$). The individual MS/MS spectrum with the statistically significant (confidence interval > 90%) best ion score (based on MS/MS spectra) was accepted. The identified proteins were then matched to specific processes or functions by searching Gene Ontology (<http://www.geneontology.org/>).

2.7. Quantitative real-time PCR assays

Total liver RNA was extracted from frozen liver tissues using TRIZOL reagent (Invitrogen Corp., Carlsbad, CA) according to manufacturer's instructions. The concentration was measured by absorbance at 260 nm using a UV1240 spectrophotometer (Shimadzu, Japan). The purity was assessed by determining the A_{260}/A_{280} ratio. The cDNA was then synthesized via reverse transcription (RT) using an oligo-(dT)₁₅ primer

and the M-MuLV reverse transcriptase (Promega, Madison, USA) in accordance with manufacturer's recommendations. Real-time PCR reactions were performed with the Stratagene Mx3000P qPCR system (Stratagene, USA). The SYBR Green PCR Master Mix reagent kits (Tiangen, Beijing, China) were used according to the manufacturer's instructions for quantification of gene expression. Zebrafish-specific primers were designed for the genes of interest using Primer Premier 5.0 software (Table S2, Supplementary data). The housekeeping gene hypoxanthine guanine phosphoribosyltransferase (HPRT) was used as an internal control. The differences in efficiencies of amplification between the target genes and HPRT were all less than 5%. The PCR amplification protocol was as follows: 95 °C for 2 min followed by 40 cycles of 94 °C for 15 s, 56 °C for 15 s, and 72 °C for 10 s. Quantification of the transcripts was performed using the $2^{-\Delta\Delta C_t}$ method (Pfaffl, 2001).

2.8. Statistical analysis

Raw data were analyzed using SPSS for Windows 13.0 Software (SPSS, Inc., Chicago, IL) and presented as means with standard errors (mean ± SE). Differences between the control and the treatment groups were determined using a one-way analysis of variance (ANOVA) followed by the Ducana multiple range test. A p -value of < 0.05 was considered statistically significant.

3. Results and discussion

Hepatotoxicity in male zebrafish following chronic PFNA exposure was evaluated for histopathological changes and transcriptional and translational effects. Comprehensive evaluation using these techniques may provide a useful tool for safety assessment of toxicity in the liver.

3.1. Hepatic histopathology

Compared to the control fish (Fig. 1A), the hepatic parenchyma of the 0.1 mg/L PFNA treated sample was less homogenous, with uneven staining intensity of eosin observed.

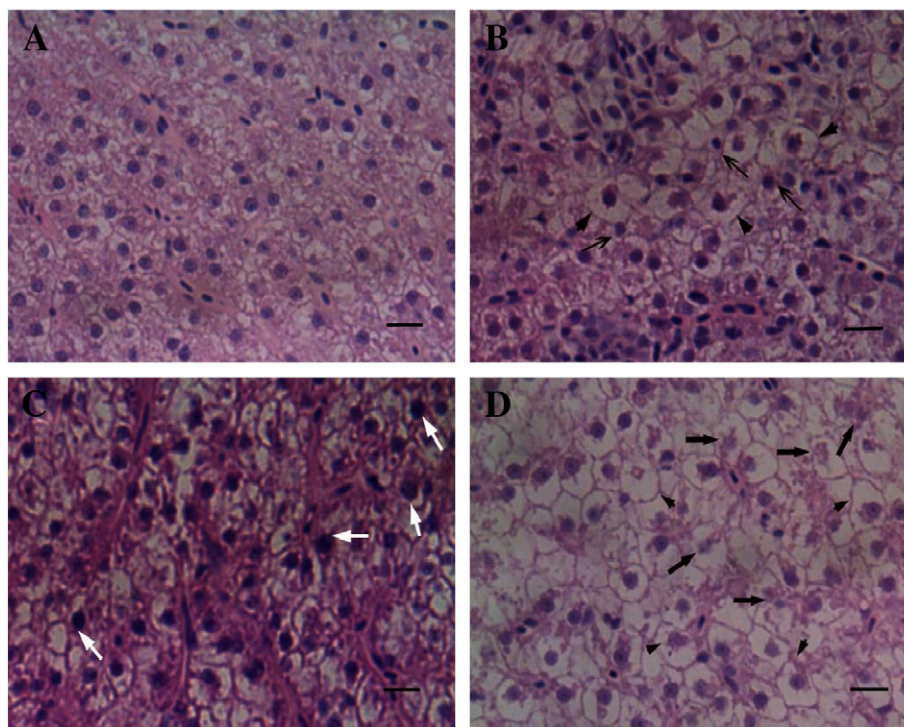


Fig. 1. Liver histopathology of male zebrafish after exposure to PFNA for 180 days. Photomicrographs of liver sections (4–5 μm) stained with hematoxylin and eosin. (A) Livers from control group. (B) Livers from fish exposed to 0.1 mg/L PFNA. A number of hepatocytes were swollen (arrowhead). Nuclei pycnosis (arrows) was observed. (C) Livers from fish exposed to 0.5 mg/L PFNA. Karyomegaly was noted (white solid arrows). (D) Livers from fish exposed to 1.0 mg/L PFNA. Decrease in cytoplasmic eosinophilia, swelling of hepatocytes (arrowhead), and karyolysis (solid arrows) was observed. Scale bar is equal to 20 μm.

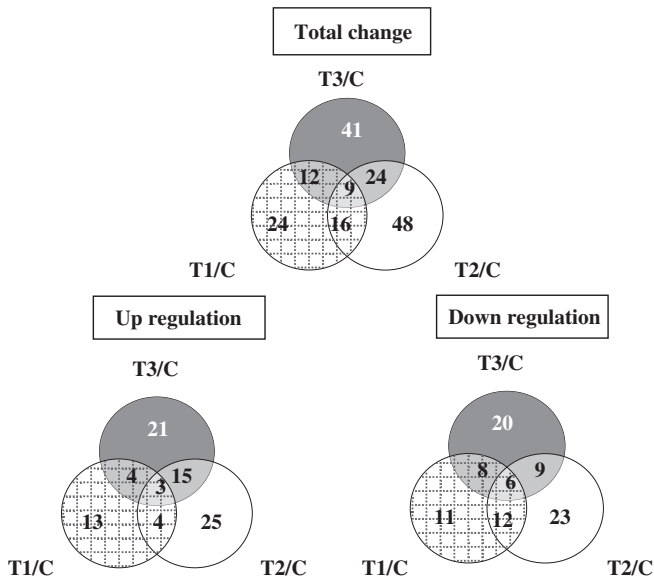


Fig. 2. The differentially expressed proteins in the zebrafish livers from the control (C) and treatment groups (T). T1, T2 and T3 indicate 0.1, 0.5 and 1.0 mg/L of PFNA-treated groups, respectively.

Swelling of hepatic cells and nuclei pycnosis was also observed in the 0.1 mg/L group (Fig. 1B). Karyomegaly and hepatocyte swelling was observed in the 0.5 mg/L PFNA treated sample (Fig. 1C). An obvious decrease in cytoplasmic eosinophilia was observed in the 1.0 mg/L group, indicating cytopathological alterations of the hepatocytes. Cell swelling was more obvious and severe nuclear anomaly of karyolysis was also observed in the 1.0 mg/L group (Fig. 1D). These observations

were similar to the effects of PFAAs reported by most previous studies (Kennedy et al., 2004; Seacat et al., 2003). Our results indicate that PFNA elicited obvious hepatic lesions, which became more severe with increasing PFNA concentrations.

3.2. Hepatic protein profiles by 2-D DIGE

The liver samples were analyzed via 2-D DIGE to investigate the alteration of protein expression following long-term PFNA exposure. After matching, 174 spots showed significant variations between the control and treatment groups: BVA module analysis showed that 61, 97, and 86 spots were significantly altered in the 0.1, 0.5, and 1.0 mg/L PFNA groups, respectively ($p < 0.05$). Nine proteins were significantly altered in the three treatments. In total, 85 proteins (24 for 0.1 mg/L, 47 for 0.5 mg/L, and 43 for 1.0 mg/L) were up-regulated and 89 proteins (37 for 0.1 mg/L, 50 for 0.5 mg/L, and 43 for 1.0 mg/L) were down-regulated compared to the control (Fig. 2). From the 134 selected spots excised from silver-stained gels, 57 proteins were successfully identified with C.I.% values greater than 90% using MALDI-TOF-MS/MS analysis ($p < 0.05$) (Fig. 3). The matched proteins came from the NCBI database for zebrafish (*Danio rerio*), and their name, accession number, MW, pI, change in relative abundance, and other MS data are summarized in Table 1.

3.3. The classification of identified proteins by functional categories

After proteomic analysis, the 57 successfully identified proteins were found to be involved in various biological activities, such as metabolism (18 proteins), structure and motility (10 proteins), stress and defense (6 proteins), signal transduction (5 proteins), cell communication (4 proteins), mitochondrial energy metabolism (4 proteins), immune response (2 proteins), response to oxidative stress (2 proteins), gene expression and regulation (1 protein), transport (1 protein), cell cycle regulation (1 protein), and other functions (3 proteins) (Fig. 4A).

Of the proteins relevant to metabolism, functions included protein metabolism and modification (5 proteins), gluconeogenesis and glycolysis (3 proteins), amino acid metabolism (2 proteins), nucleotides metabolism (2 proteins), TCA cycle and pyruvate metabolism (1 protein), and other metabolism (5 proteins). Close to a third of the proteins were involved in protein metabolism and modification (Fig. 4B). Of these, ubiquitin specific protease 5 (USP5) was significantly increased in all PFNA-treated groups. USP5 disassembles branched polyubiquitin chains into ubiquitin monomers on degraded proteins in the late stage of the ubiquitin-dependent proteolysis process, which helps to maintain chromatin structure, receptor function, and degradation of abnormal proteins (Wilkinson et al., 1995). This result suggests that the activation of self-protection

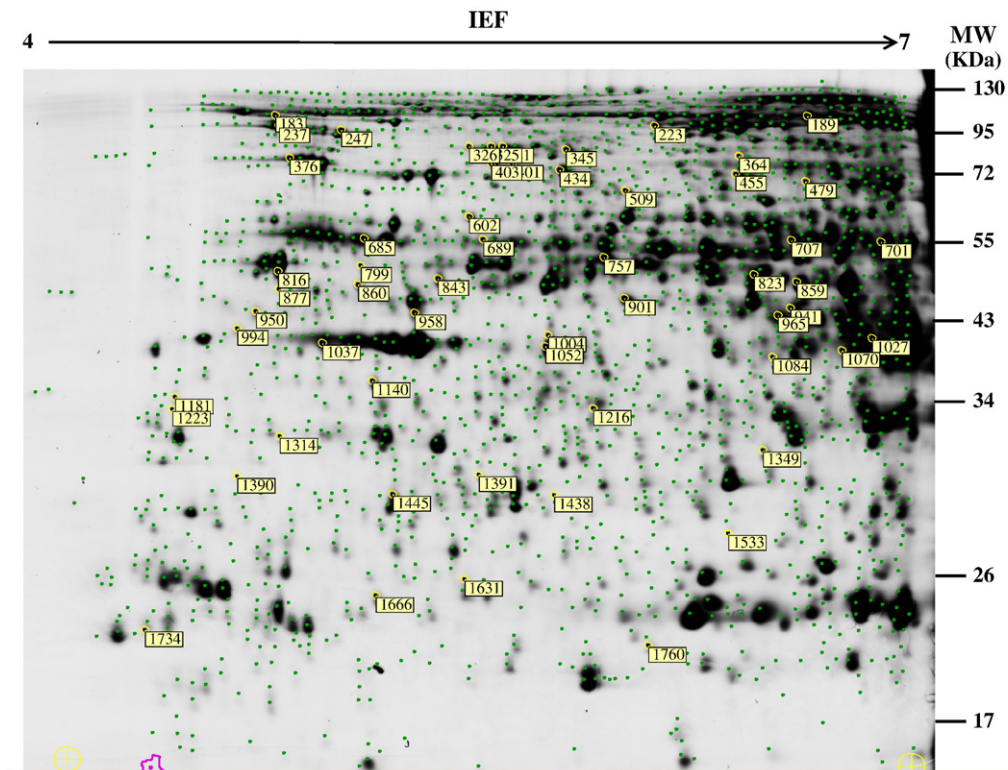


Fig. 3. Representative two-dimensional difference gel electrophoresis (2-D DIGE) maps of the proteome of PFNA-treated zebrafish livers between pH 4 and 7. Delimited spots correspond to proteins of interest selected for mass spectrometry identification. ID of identified proteins from Table 1 is indicated in yellow boxes.

Table 1
Differentially expressed proteins in liver from control and PFNA-treated zebrafish.

Spot ID	NCBI	Protein name	Protein score	Sequence ^a	Theoretical MW	Theoretical pI	Fold change induced by PFNA (mg/L) ^b			Functional category
							0.1	0.5	1.0	
Metabolism (18)										
<i>Amino acid metabolism (2)</i>										
223	gi 161612168	Dmgdh protein	118		97386.4	6.54	1.27	1.40*	1.35*	Glycine catabolism
1027	gi 31419240	Ckmb protein	214	GTGGVDTASVGGVFDISNADR	42824.5	6.29	-4.89*	-5.29*	-1.74	Arginine catabolism/proline catabolism/ ATP binding/nucleotide binding/transferase/ transferring phosphorus-containing groups
<i>TCA cycle and pyruvate metabolism (1)</i>										
1037	gi 33989739	Suclg2 protein	190		45221.6	5.57	-1.15*	-1.12	-1.08	TCA cycle/propanoate metabolism
<i>Gluconeogenesis and glycolysis (3)</i>										
823	gi 94574478	Aldh2b protein	144	TFVQESIYDEFVER	56422.4	6.35	1.05	1.82	2.26*	Glycolysis/gluconeogenesis/alcohol metabolism/ oxidation reduction
859	gi 47551317	Enolase 3, (beta, muscle)	231	AAVPSGASTGVHEALELR	47442.3	6.25	1.18	-1.24*	-1.22*	Glycolysis/gluconeogenesis/fructose and mannose metabolism/pentose phosphate pathway
1070	gi 35902900	Fructose-bisphosphate aldolase C	74		39234.9	6.21	-1.26*	-1.36*	-1.27*	
<i>Protein metabolism and modification (5)</i>										
183	gi 44890334	Ubiquitin specific protease 5	131		92755.5	4.91	1.26*	1.26*	1.27*	Ubiquitin-dependent protein catabolism
345	gi 66910298	Si:dkey-276i5.1 protein	109		86251.9	6.80	1.26*	1.16	1.23*	Glycyl-tRNA aminoacylation for protein translation/ Protein biosynthesis
509	gi 220678632	Novel protein similar to vertebrate asparaginyl-tRNA synthetase (NARS)	134		63784.0	5.79	1.14	1.18*	1.16	Asparaginyl-tRNA biosynthesis
877	gi 38198661	DNA-damage inducible protein 2	96		45242.0	4.90	1.09	1.04	1.19*	Proteolysis (aspartic-type endopeptidase)/ protein modification
1390	gi 50540062	Otubain 1	86		29273.6	5.07	1.34	1.13	1.17*	Cysteine proteases,providing an editing function for polyubiquitin chain growth
<i>Nucleotides metabolism (2)</i>										
1052	gi 27882111	Adka protein	94	AGHYAANVIIR	37420.7	5.43	1.31	1.17	1.32*	Purine metabolism/purine ribonucleoside salvage
1760	gi 150383502	UMP-CMP kinase/cytidylate kinase/ deoxycytidylate kinase	136	IVENYSYTHLSAGDLLR	22409.3	5.46	1.37*	1.19	1.24	Pyrimidine nucleotide biosynthesis/nucleobase, nucleoside,nucleotide and nucleic acid metabolism
<i>Other metabolism (5)</i>										
189	gi 125819811	LOC798292 similar to 10-formyltetrahydrofolate dehydrogenase (10-FTHFDH) (Aldehyde dehydrogenase family 1 member L1)	155		100117.3	6.17	1.61	1.69*	1.09	One carbon pool by folate
701	gi 190337470	Ugdh protein	163	IPFTTSGGVPR	54513.0	6.37	1.37	1.48	2.00*	Amino sugar and nucleotide sugar metabolism/ ascorbate and aldarate metabolism/pentose and glucuronate interconversions/starch and sucrose metabolism/oxidation reduction
757	gi 115497492	Hypothetical protein LOC767699	102		56862.2	5.88	1.50	1.39	1.99*	Metabolism (methyltransferase activity)
1349	gi 62005995	Sult1 isoform 6	157	AVFDQSISAFMR	35588.9	6.19	1.19	1.06	1.32*	Estrone sulfotransferase/steroidogenesis
1666	gi 41053646	Glutathione S-transferase theta 1b	60		27989.7	7.71	1.36	1.44	1.91*	Detoxification/transferase
<i>Stress and defense (6)</i>										
237	gi 226823315	Heat shock protein 90 kDa alpha, class B member 1	228	HFSVEGQLEFR	83305.0	4.90	1.20	1.42*	1.32*	Protein folding/response to stress
376	gi 39645428	Heat shock protein 5	135	DNHLLGTFDLTGIPPAPR	71946.2	5.04	-1.10	1.17*	-1.01	Response to stress

434	gi 28278640	Heat shock protein 9	294	NAVVTVPAYFNDSQR	73848.0	7.06	1.25*	1.24	1.15	Protein folding/response to stress/hemopoiesis
602	gi 47086803	Chaperonin containing TCP1, subunit 5 (epsilon)	75		59356.9	5.39	1.13	1.20*	1.10	Protein folding/cellular protein metabolism
1004	gi 38488745	DnaJ (Hsp40) homolog, subfamily B, member 11	88		40777.8	5.63	1.02	1.06	1.10*	Protein folding
1533	gi 189518348	PREDICTED: similar to zinc finger protein 228	63		30788.0	8.63	1.15	1.46*	-1.00	
<i>Structure and motility (10)</i>										
321	gi 66472810	Ezrin like	198		70053.6	5.42	1.65	1.68	1.65*	Cytoskeleton
325	gi 66472810	Ezrin like	232	APDFVFYASR	70053.6	5.42	1.64	1.78	2.00*	Cytoskeleton
326	gi 66472810	Ezrin like	120		70053.6	5.42	1.43	1.75*	1.84*	Cytoskeleton
364	gi 18858919	Junction plakoglobin	88		79982.3	5.89	1.27	1.29*	1.11	Cell adhesion/negative regulation of Wnt receptor signaling pathway involved in heart development
799	gi 189531224	PREDICTED: filamin A interacting protein 1	63		132334.8	6.37	1.53	1.52*	1.31	Interact with filamin
941	gi 116875789	Hypothetical protein LOC768289	75		47729.2	6.11	-1.57*	-1.70*	-1.74*	Structural molecule activity
965	gi 116875789	Hypothetical protein LOC768289	81		47729.2	6.11	1.35	1.28*	1.42*	Structural molecule activity
950	gi 157423081	Zgc:77517 protein	79		44051.0	4.94	-1.27	-1.21	-1.30*	Structural molecule activity
1181	gi 28277767	Tpm1 protein	226	KLVIVEGELER	32729.7	4.69	-127.40*	-54.30*	-2.18	Cardiac muscle contraction (tropomyosin 1 alpha chain)
1734	gi 41053385	Fast skeletal myosin alkali light chain 1	132		20918.4	4.63	-3.36*	-3.88*	-2.56	Calcium ion binding
<i>Cell communication (4)</i>										
685	gi 41056085	Keratin 8	274	NLDMDAIVAEVR	57723.4	5.15	-1.26*	-1.23	-1.18	Membrane organization/signal transduction/calcium binding
689	gi 39645432	Krt5 protein	242	AIFEEELR	57792.3	5.27	-5.48*	-4.88*	-3.76*	Membrane organization/signal transduction/calcium binding
843	gi 51010971	Keratin 12	270		49963.6	5.31	-4.19*	-2.99	-4.04*	Membrane organization/signal transduction/calcium binding
860	gi 47087241	Keratin 15	70		49093.4	5.13	-2.32*	-1.92	-2.87*	Membrane organization/signal transduction/calcium binding
<i>Immune response (2)</i>										
247	gi 220941693	Complement component 9	111	AGYGINILGSGPR	72666.8	5.36	-2.14*	-1.93*	-1.96*	Response to chemical stimulus
455	gi 189546565	PREDICTED: similar to complement component c3b, partial	68	VGSENVFVEAQDYSGEPLR	101171.5	5.78	-1.83*	-1.69	-ECHS11.82	Response to chemical stimulus
<i>Mitochondrial energy metabolism (4)</i>										
401	gi 56090150	NADH dehydrogenase (ubiquinone)Fe-S protein 1	69		79382.4	5.82	1.27*	-1.00	1.08	ATP synthesis coupled electron transport/oxidation reduction
403	gi 56090150	NADH dehydrogenase (ubiquinone) Fe-S protein 1	235	FASEVAGVEDLGTGTR	79382.4	5.82	1.31	1.30*	1.37*	ATP synthesis coupled electron transport/oxidation reduction
816	gi 189525553	PREDICTED: mitochondrial ATP synthase beta subunit, partial	473	IPSAVGYQPTLATDMGTMQER	55095.8	5.14	-1.10	-1.21*	-1.18	ATP synthesis/metabolism/oxidative phosphorylation
901	gi 47123260	Ubiquinol-cytochrome c reductase core protein I	118		52079.2	6.18	1.14*	1.13*	1.12	Electron transport/proteolysis
<i>Signal transduction (5)</i>										
1084	gi 157422762	Anxa3b protein	62		37616.3	5.13	1.28*	1.05	1.07	Regulation of cellular growth and signal transduction pathways
1140	gi 157422762	Anxa3b protein	64		37616.3	5.13	1.01	1.75*	1.42*	Regulation of cellular growth and signal transduction pathways
1216	gi 123208289	Annexin A1a	63		25368.1	5.38	-1.46	-2.46*	-2.20*	Calcium-dependent phospholipid binding
1391	gi 27762270	Annexin 5	210	YGTDEGQFITILGNR	35036.0	5.46	-3.42	-2.43	-3.66*	Negative regulation of coagulation
1438	gi 57524661	MAWD binding protein-like	71	GAPNAQPGYDFYSR	31690.2	5.89	1.30	-5.48*	-1.79	Biosynthesis

(continued on next page)

Table 1 (continued)

Spot ID	NCBI	Protein name	Protein score	Sequence ^a	Theoretical MW	Theoretical pI	Fold change induced by PFNA (mg/L) ^b			Functional category
							0.1	0.5	1.0	
<i>Gene expression and regulation (1)</i>										
958	gi 38198643	Eukaryotic translation initiation factor 4A, isoform 1A	97	GIDVQQVSLVINYLPTNR	46223.7	5.26	−1.01	1.11*	1.01	Translation
<i>Transport (1)</i>										
707	gi 162287365	Hemopexin	153	VHLDAITSDDAGNIYAFR	50965.7	6.18	−1.23	−1.48	−1.76*	Transport
<i>Response to oxidative stress (2)</i>										
994	gi 169646767	Glutathione peroxidase 4b	68		21523.7	8.65	−1.76	−1.63	−1.77*	Oxidation reduction/response to oxidative stress
1314	gi 125852445	PREDICTED: hypothetical protein	130	VIGNSDFQAEISGAGSR	32010.7	4.78	1.11	1.17*	1.19*	
<i>Cell cycle regulation (1)</i>										
1631	gi 47085905	Tyrosine 3-monooxygenase/tryptophan 5-monooxygenase activation protein, beta polypeptide 2	66		27375.5	4.68	−1.12*	−1.11	−1.07	Protein domain specific binding, cell cycle
<i>Other function (3)</i>										
479	gi 68397162	PREDICTED: wu:fi47e11 isoform 1	64		58560.5	9.58	−2.07	−1.68	−2.35*	
1223	gi 156616350	Hypothetical protein LOC100124602	86		28791.8	4.83	−19.31	−21.95*	−3.72	
1445	gi 220678692	Novel protein similar to vertebrate phenazine biosynthesis-like protein domain containing (PBLD, zgc:112210)	88		31705.2	5.51	1.56	1.34*	−1.09	

^a The sequence of matched peptides identified by MS/MS (ion cross confidence interval CI%>90%).

^b Fold-changes were calculated by comparing the intensity of protein between control and treatment samples ($n = 3$).

* $p < 0.05$.

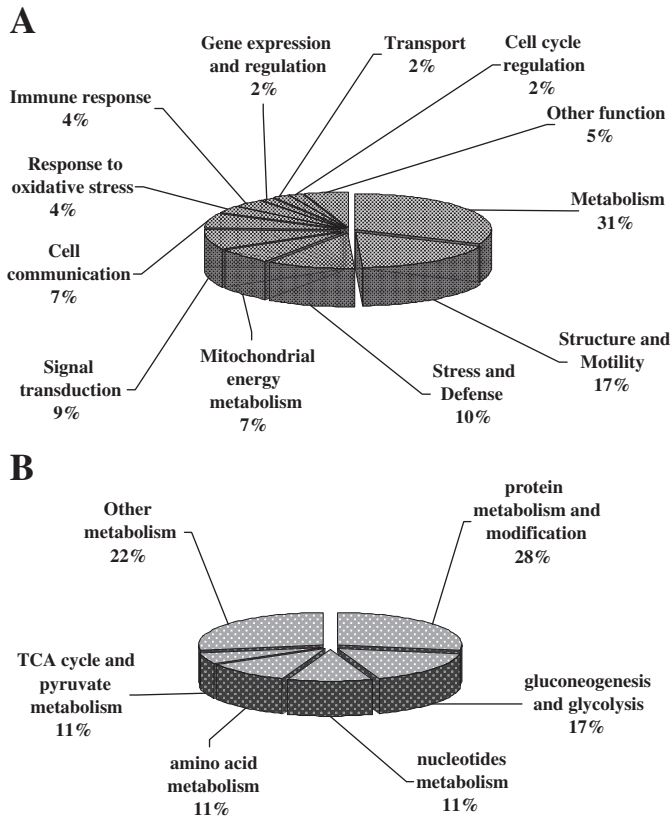


Fig. 4. Pie chart distribution of protein identities based on (A) function of the proteins and (B) function of the proteins relevant to metabolism.

mechanisms to survive PFNA exposure is achieved by removing increased production of damaged proteins or organelles.

The second largest category proteins were from the cytoskeleton, which was implicated in morphological changes and molecular trafficking. These proteins included ezrin-like, junction plakoglobin, filamin A interacting protein 1 (PREDICTED), Tpm1 protein, and fast skeletal myosin alkali light chain 1. Reduced expression of these proteins suggests that cytoskeleton reorganization may be involved in the toxic effects on hepatic function induced by PFNA. It may also cause significant disruption to cytoskeleton organization in the hepatocytes through hepatic cell swelling and nuclear karyolysis.

From our results, aldehyde dehydrogenase 2b (ALDH2b) and SULT1 isoform 6 were significantly increased in the 1.0 mg/L PFNA group. Glutathione S-transferase theta 1b (GSTT1b) displayed a generally consistent upregulated trend in all PFNA-treated groups. Previous research has shown that cells contain a number of antioxidant, antioxidant, and anti-inflammatory defenses (Cerutti and Trump, 1991; Mates and Sanchez-Jimenez, 1999), including the involvement of ALDH2, SULTs, and GSTs in cellular detoxification. ALDH2, for example, functions in the mitochondria and possesses an NAD⁺-linked activity responsible for detoxification of short-chain aldehydes to the corresponding acids in vivo (Song et al., 2006); glutathione S-transferases (GSTs) are phase II detoxification enzymes involved in the metabolism of carcinogens and anticancer drugs and their interaction with kinase complexes during oxidative or chemical stress-induced apoptosis (Voso et al., 2008); and SULTs are major phase II enzymes involved in the biotransformation of endogenous chemicals, such as steroid thyroid hormones, and in the detoxification of environmental xenobiotics in animals (Gamage et al., 2006). Our results indicate that these three enzymes were more sensitive to PFNA than other proteins analyzed in this study, and their significant up-regulation suggests increased production of reactive oxygen species (ROS) in the liver and activation of self-protection mechanisms.

The four proteins involved in the mitochondrial respiratory chain, including NADH dehydrogenase (ubiquinone) Fe-S protein 1 and ubiquinol-cytochrome c reductase core protein 1, were significantly up-regulated in response to PFNA treatment. These proteins play important roles in mitochondrial electron transport. Additionally, it has been demonstrated that mitochondria respiratory activity always parallels production of ROS (Zamzami et al., 2005), and abnormal mitochondrial respiration produces abundant ROS. If these ROS from the intermembrane of mitochondria are not fully cleared by antioxidant defense system, the oxidative stress response will be initiated and will cause mitochondrial DNA damage or cell death (Orrenius et al., 2007). Our results imply that mitochondrial disruption and oxidative stress may play important roles in hepatic damage induced by PFNA exposure.

An important group of molecular chaperones associated with the mitochondria, including heat shock protein (HSP) 90 kDa alpha, class B member 1, heat shock protein 5, heat shock protein 9, chaperonin containing TCP1 subunit 5 (epsilon), DnaJ (Hsp40) homolog subfamily B, member 11, and similar to zinc finger protein 228 (PREDICTED), were all up-regulated. Heat shock proteins are well-known anti-stress proteins that regulate protein

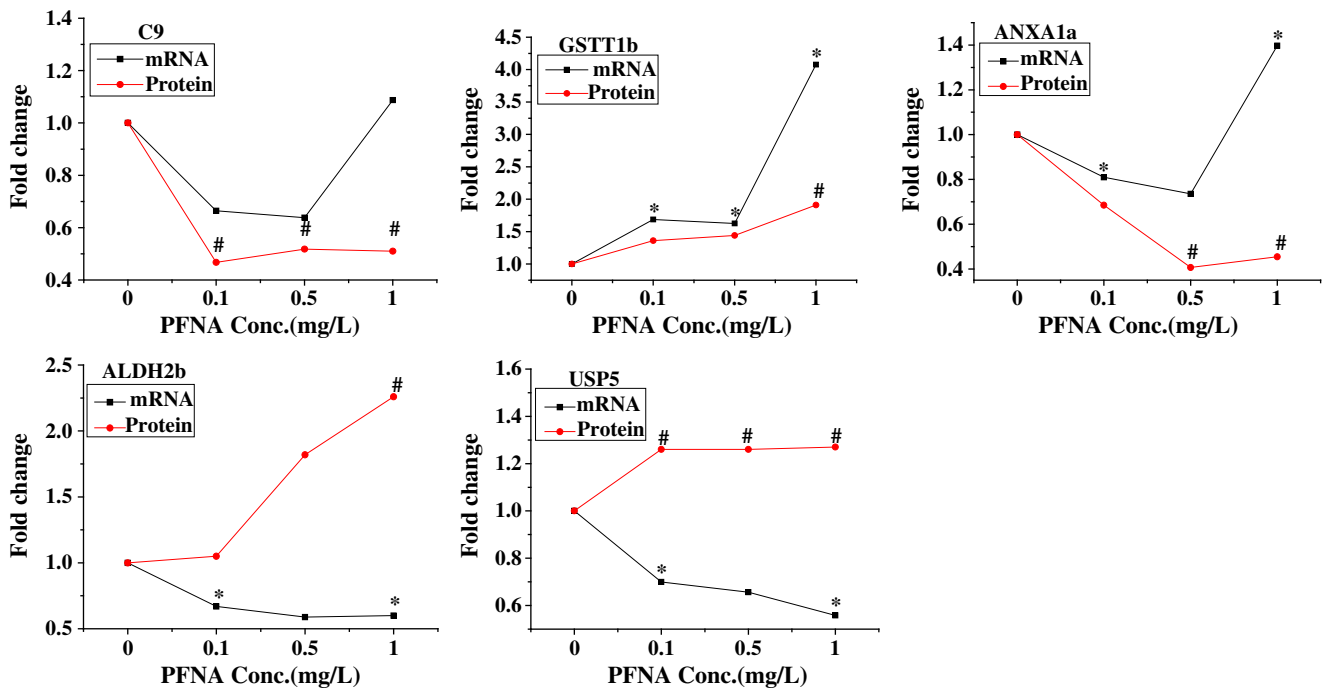


Fig. 5. The alteration of protein and mRNA expression of selected altered proteins in the livers of male zebrafish following PFNA treatments. The line charts show the protein levels based on 2-D DIGE and mRNA levels using real-time PCR analysis. The values represent average fold changes. The values of protein abundance are the average % volume of spots in three replicated gels. Significant changes of mRNA levels compared to the controls ($p < 0.05$) are indicated by asterisks (*). The pound sign (#) refers to an average increase or decrease in protein levels compared to the controls ($p < 0.05$).

turnover and assembly and protect cells from harmful conditions, including oxidative stress (Jullig et al., 2007). The over-expression of HSPs usually correlates with harmful insults to the cell (Kiang and Tsokos, 1998). Our results suggest that oxidative stress may occur due to hepatic toxicity from PFNA exposure and that HSPs may offer a functional protective advantage.

We also identified a pool of annexins (annexin III, annexin V, and annexin A1a), which are water soluble proteins that function as Ca^{2+} channels and regulate membrane fusion, a process underlying organelle biogenesis and cell division (Kourie and Wood, 2000). Although in vitro annexins exhibit anti-inflammatory and tumor suppression activities (Benz and Hofmann, 1997), its physiological function in vivo is largely unknown (Kourie and Wood, 2000). In fish leukocytes, ANX4 increased the permeability and fluidity of cell membranes and affected mitochondrial membrane potential (Hu et al., 2003). Additionally, studies on cultured cells exposed to PFCs have shown that the dissipation of plasma membrane potential can lead to cytosol acidification (Kleszczynski and Skladanowski, 2009). Therefore, the downregulation of ANXA1a and ANX5 may be associated with PFNA-mediated dysregulation of the cell membrane function, although further research is warranted to demonstrate this association.

Taken together, aberrant increases in the levels of proteins related to stress, detoxification, and anti-oxidation in PFNA-treated groups showed the stimulation of cell defense systems in response to PFNA stimuli. Proteomic analysis provided insight into the hepatotoxicity of PFNA, and helped clarify understanding of these proteins, which provides a strong basis to investigate the importance of PFNA in chemical risk assessment.

3.4. The relationship between transcription and translation

To verify the 2-D DIGE results and compare the correlation between protein expression and gene expression, we examined the expression of five genes: complement component 9 (C9), ANXA1a, GSTT1b, ALDH2b, and USP5, which are related to immune response, signal transduction, metabolism, and protein modification, respectively. The trend of mRNA levels in C9, GSTT1b, and ANXA1a were similar to the changes observed for their protein levels. Although the gene expression of C9 and ANXA1a increased in the 1.0 mg/L PFNA group compared to the control, this increase was not significant ($p > 0.05$, Fig. 5). However, different trends occurred with ALDH2b and USP5 mRNA expression levels compared to their protein expression. The mRNA levels of ALDH2b and USP5 dramatically decreased in the 0.1 and 1.0 mg/L PFNA treatment groups compared to the control, though the protein level of ALDH2b increased in the 1.0 mg/L treatment group and the protein level of USP5 in three treatment groups was significant ($p < 0.05$, Fig. 5), respectively. These results suggest that the relationship between mRNA transcription and protein translation is not always a direct regulatory mechanism, and the gene expression response to PFNA may have diverse regulatory mechanisms from transcription of mRNA to the formation of functional proteins. In general, it would be better to integrate the advantages of transcriptional and protein's analysis.

3.5. PPARs and PPAR α target genes expression

To confirm if the hepatotoxicity mechanism between PFNA and other PFAAs is the same, the transcriptional levels of PPARs and several downstream PPAR α genes were analyzed. As three types of PPARs have been identified in zebrafish: α , δ , and γ (Ibabe et al., 2002), we examined the transcriptional levels of PPAR α (a and b), PPAR δ (a and b) and PPAR γ in zebrafish liver (Fig. 6A). Compared to the control group, no marked differences in the mRNA levels were exhibited between any groups except for PPAR α b, which was reduced 2.8-fold in the 1.0 mg/L PFNA group ($p < 0.01$). The PPAR α a level reduced at all doses, while the PPAR δ (a and b) level increased at all doses, although the differences were not statistically significant ($p > 0.05$). Similarly, although the levels of PPAR γ increased at PFNA doses of 0.1 and 0.5 mg/L and decreased at doses of 1.0 mg/L, no significant change occurred in the expression of PPAR γ ($p > 0.05$) (Fig. 6A).

The mRNA levels of six important PPAR α target genes (long chain acyl-CoA thioester hydrolase, CTE; hydroxyacyl-Coenzyme A dehydrogenase, HADHA; acyl CoA oxidase, ACOX; carnitine palmitoyltransferase 1 and 2, CPT1 and CPT2; and mitochondrial enoyl coenzyme A hydratase 1, ECHS1) were also investigated (Fig. 6B). Consistent with the level of PPAR α , the differences in the six genes were not statistically significant, except for the obvious down-regulated expression of CPT2 observed for the 1.0 mg/L PFNA treatment group ($p < 0.01$) compared to the control. Importantly, CPT2, which is a nuclear protein and transported to the mitochondrial inner membrane, oxidizes long-chain fatty acids with CPT1 in the mitochondria. Defects in this gene are associated with mitochondrial long-chain fatty-acid oxidation disorders and carnitine palmitoyltransferase II deficiency (Bonnefont et al., 1999). In addition, the CPT system plays a pivotal role in fatty acid oxidation and energy production by catalyzing the transfer of palmitate from the cytosol to the mitochondrial matrix (McGarry and Brown, 1997). Our results indicate that CPT2 was more sensitive to PFNA than CPT1 as a PPAR α target gene, and depression of CPT2 expression may lead to decreased entry of fatty acids and mimics into the mitochondria, resulting in decreased energy supply.

Both PPAR α and PPAR γ are key regulators of lipid homeostasis and can be activated by a structurally diverse group of compounds. Target genes are transactivated by PPARs upon binding to peroxisome proliferator-response elements (PPREs) through heterodimerization with retinoid X receptor (RXR) (Kliewer et al.,

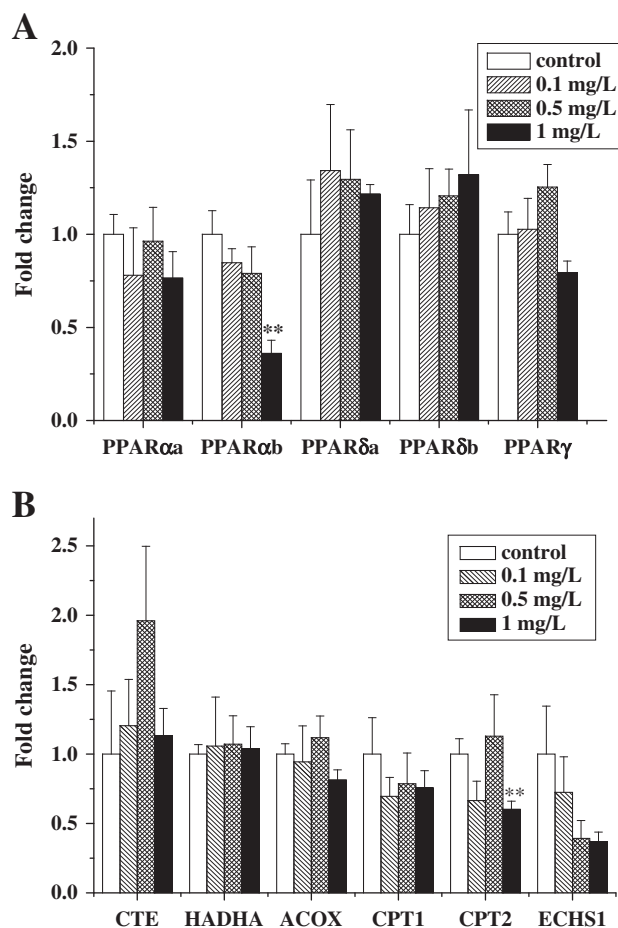


Fig. 6. Real-time quantitative PCR analyses of hepatic mRNA expression levels of (A) PPAR α (a and b), PPAR δ (a and b), and PPAR γ ; and (B) CTE, HADHA, ACOX, CPT1, CPT2, and ECHS1 from control and PFNA-exposed male zebrafish. Gene expression levels represent the relative mRNA expression compared to controls. Values are presented as the mean \pm SEM for six zebrafish per group. Double asterisks (**) indicate a highly significant difference, $p < 0.01$.

1992). In response to ligand activation, all PPAR isoforms (PPAR α , PPAR β/δ and PPAR γ) bind to PPREs as heterodimers with RXR. This binding modulates the expression of target genes involved in lipid metabolism and synthesis, such as ACOX, CPT1, and CYP4A1 (Shearer and Hoekstra, 2003), as well as MTE, CPT2, CTE, HADHA, and ECH1.

Perfluorocarboxylic acids (PFCAs) have a structure similar to endogenous fatty acids, except that fluorine atoms replace the hydrogen atoms. Therefore, PFCAs could potentially be mistaken as a substrate by the fatty acid metabolism machinery due to structural similarity with endogenous fatty acids. Previous research has indicated that PFOA exposure in rodents leads to changes typically associated with peroxisome proliferator chemicals, including increases in fatty acid β -oxidation enzymes and liver-to-body weight ratios (Kudo et al., 2000). The effects of PFOA on liver are assumed to be mediated by PPAR α (Kennedy et al., 2004).

The upregulated expression of both PPAR α and PPAR γ was a characteristic finding in rats treated with PFDoA (Zhang et al., 2008). Both PPAR α and PPAR γ and their downstream genes also show the same upregulated trends in rat livers treated with PFNA. Furthermore, differential enzymes such as CTE, MTE, and ECH1 involved in lipid metabolism in rat livers were detected by 2-D-DIGE and identified by MALDI TOF/TOF (unpublished data). Interestingly, in our study no significant differences in the mRNA levels of PPARs were exhibited among any groups except for PPAR α b, which was significantly reduced in male zebrafish exposed to 1.0 mg/L PFNA. This result was similar to our previous study, which showed that subacute exposure of zebrafish to PFDoA produced a dramatic decrease in PPAR α expression (Liu et al., 2008). No differential expression proteins involved in the lipid homeostasis or the PPAR downstream target were detected in the current study. This may be due to species-specific responses to peroxisome proliferators, particularly as rodents are extremely sensitive to peroxisome proliferators compared to other species (Bentley et al., 1993; Youssef and Badr, 1998). The mechanism related to the different responses of rodents and non-rodents to peroxisome proliferators is not fully understood. Although most studies have indicated that the hepatotoxicity of PFCAs is related to the activation of

PPARs, the present results suggest that the PPAR α -independent pathways altered by PFCAs, such as the constitutive androstane receptors and the pregnane X receptors involved in xenobiotic metabolism and phase I, II, and III processes, should not be discounted.

In summary, our proteomic analyses provide new perspective to the hepatotoxicity of PFNA in teleosts. The extensive protein variations indicate that multiple cellular pathways were involved and suggest that multiple protein molecules should be simultaneously targeted as an effective strategy to counter PFNA exposure. The present findings also demonstrated that PPARs could not sufficiently explain all toxic effects of PFAAs. Further investigations are required to elucidate the potential PPAR independent pathways involved in PFAA liver toxicity in fish.

Acknowledgment

This research was supported by the National Natural Science Foundation of China (Grant #s 31025006 and 20837004).

Appendix A. Supplementary data

Supplementary data to this article can be found online at doi:10.1016/j.envint.2011.03.002.

References

- Bentley PK, Johnson OL, Washington C, Lowe KC. Uptake of concentrated perfluorocarbon emulsions into rat lymphoid-tissues. *J Pharm Pharmacol* 1993;45:182–5.
- Benz J, Hofmann A. Annexins: from structure to function. *Biol Chem* 1997;378:177–83.
- Bonnefont JP, Demaugre F, Prip-Buus C, Saudubray JM, Brivet M, Abadi N, et al. Carnitine palmitoyltransferase deficiencies. *Mol Genet Metab* 1999;68:424–40.
- Calafat AM, Wong LY, Kuklennyik Z, Reidy JA, Needham LL. Polyfluoroalkyl chemicals in the US population: data from the National Health and Nutrition Examination Survey (NHANES) 2003–2004 and comparisons with NHANES 1999–2000. *Environ Health Persp* 2007;115:1596–602.
- Cerutti PA, Trump BF. Inflammation and oxidative stress in carcinogenesis. *Cancer Cell Mon Rev* 1991;3:1–7.
- Dinglasan-Panlilio MJA, Mabury SA. Significant residual fluorinated alcohols present in various fluorinated materials. *Environ Sci Technol* 2006;40:1447–53.
- Gamage N, Barnett A, Hempel N, Duggleby RG, Windmill KF, Martin JL, et al. Human sulfotransferases and their role in chemical metabolism. *Toxicol Sci* 2006;90:5–22.
- Guruge KS, Taniyasu S, Yamashita N, Wijeratna S, Mohotti KM, Seneviratne HR, et al. Perfluorinated organic compounds in human blood serum and seminal plasma: a study of urban and rural tea worker populations in Sri Lanka. *J Environ Monit* 2005;7:371–7.
- Guruge KS, Yeung LWY, Yamanaka N, Miyazaki S, Lam PKS, Giesy JP, et al. Gene expression profiles in rat liver treated with perfluorooctanoic acid (PFOA). *Toxicol Sci* 2006;89:93–107.
- Hart K, Gill VA, Kannan K. Temporal trends (1992–2007) of perfluorinated chemicals in Northern Sea Otters (*Enhydra lutris kenyoni*) from South-Central Alaska. *Arch Environ Contam Toxicol* 2009;56:607–14.
- Hekster FM, Laane RWPM, de Voogt P. Environmental and toxicity effects of perfluoroalkylated substances. *Rev Environ Contam T* 2003;179:99–121.
- Hoff PT, Van Campenhout K, Van de Vijver K, Covaci A, Bervoets L, Moens L, et al. Perfluorooctane sulfonic acid and organohalogen pollutants in liver of three freshwater fish species in Flanders (Belgium): relationships with biochemical and organismal effects. *Environ Pollut* 2005;137:324–33.
- Hoff PT, Van Dongen W, Esmans EL, Blust R, De Coen WM. Evaluation of the toxicological effects of perfluorooctane sulfonic acid in the common carp (*Cyprinus carpio*). *Aquat Toxicol* 2003;62:349–59.
- Houde M, Wells RS, Fair PA, Bossart GD, Hohn AA, Rowles TK, et al. Polyfluoroalkyl compounds in free-ranging bottlenose dolphins (*Tursiops truncatus*) from the Gulf of Mexico and the Atlantic Ocean. *Environ Sci Technol* 2005;39:6591–8.
- Hu WY, Jones PD, DeCoen W, King L, Fraker P, Newsted J, et al. Alterations in cell membrane properties caused by perfluorinated compounds. *Comp Biochem Phys C* 2003;135:77–88.
- Ibabe A, Grabenbauer M, Baumgart E, Fahimi HD, Cajaraville MP. Expression of peroxisome proliferator-activated receptors in zebrafish (*Danio rerio*). *Histochem Cell Biol* 2002;118:231–9.
- Ishibashi H, Iwata H, Kim EY, Tao L, Kannan K, Amano M, et al. Contamination and effects of perfluorochemicals in Baikal Seal (*Pusa sibirica*). 1. Residue level, tissue distribution, and temporal trend. *Environ Sci Technol* 2008;42:2295–301.
- Jensen AA, Leffers H. Emerging endocrine disrupters: perfluoroalkylated substances. *Int J Androl* 2008;31:161–9.
- Jullig M, Hickey AJ, Middleditch ML, Crossman DJ, Lee SC, Cooper GJS. Characterization of proteomic changes in cardiac mitochondria in streptozotocin-diabetic rats using iTRAQ (TM) isobaric tags. *Proteom Clin Appl* 2007;1:565–76.
- Karman A, Ericson I, van Bavel B, Darnerud PO, Aune M, Glynn A, et al. Exposure of perfluorinated chemicals through lactation: levels of matched human milk and serum and a temporal trend, 1996–2004, in Sweden. *Environ Health Persp* 2007;115:226–30.
- Kennedy GL, Butenhoff JL, Olsen GW, O'Connor JC, Seacat AM, Perkins RG, et al. The toxicology of perfluorooctanoate. *Crit Rev Toxicol* 2004;34:351–84.
- Kiang JG, Tsokos GC. Heat shock protein 70 kDa: molecular biology, biochemistry, and physiology. *Pharmacol Therapeut* 1998;80:183–201.
- Kleno TG, Leonardsen LR, Kjeldal HO, Laursen SM, Jensen ON, Baunsgaard D. Mechanisms of hydrazine toxicity in rat liver investigated by proteomics and multivariate data analysis. *Proteomics* 2004;4:868–80.
- Kleszczynski K, Skladanowski AC. Mechanism of cytotoxic action of perfluorinated acids. I. Alteration in plasma membrane potential and intracellular pH level. *Toxicol Appl Pharm* 2009;234:05–300.
- Kliwer SA, Umesono K, Mangelsdorf DJ, Evans RM. Retinoid X receptor interacts with nuclear receptors in retinoic acid, thyroid hormone and vitamin D3 signalling. *Nature* 1992;355:446–9.
- Kourie JJ, Wood HB. Biophysical and molecular properties of annexin-formed channels. *Prog Biophys Mol Bio* 2000;73:91–134.
- Kudo N, Bandai N, Suzuki E, Katakura M, Kawashima Y. Induction by perfluorinated fatty acids with different carbon chain length of peroxisomal beta-oxidation in the liver of rats. *Chem Biol Interact* 2000;124:119–32.
- Lau C, Anitole K, Hodes C, Lai D, Pfahles-Hutchens A, Seed J. Perfluoroalkyl acids: a review of monitoring and toxicological findings. *Toxicol Sci* 2007;99:366–94.
- Lau C, Butenhoff JL, Rogers JM. The developmental toxicity of perfluoroalkyl acids and their derivatives. *Toxicol Appl Pharm* 2004;198:231–41.
- Liu CS, Yu K, Shi XJ, Wang JX, Lam PKS, Wu RSS, et al. Induction of oxidative stress and apoptosis by PFOS and PFOA in primary cultured hepatocytes of freshwater tilapia (*Oreochromis niloticus*). *Aquat Toxicol* 2007;82:135–43.
- Liu Y, Wang JS, Wei YH, Zhang HX, Xu MQ, Dai JY. Induction of time-dependent oxidative stress and related transcriptional effects of perfluorododecanoic acid in zebrafish liver. *Aquat Toxicol* 2008;89:242–50.
- Mates JM, Sanchez-Jimenez F. Antioxidant enzymes and their implications in pathophysiologic processes. *Front Biosci* 1999;4:D339–45.
- McGarry JD, Brown NF. The mitochondrial carnitine palmitoyltransferase system. From concept to molecular analysis. *Eur J Biochem* 1997;244:1–14.
- Oakes KD, Sibley PK, Martin JW, MacLean DD, Solomon KR, Mabury SA, et al. Short-term exposures of fish to perfluorooctane sulfonate: acute effects on fatty acyl-CoA oxidase activity, oxidative stress, and circulating sex steroids. *Environ Toxicol Chem* 2005;24:1172–81.
- Oakes KD, Sibley PK, Solomon KR, Mabury SA, Van Der Kraak GJ. Impact of perfluorooctanoic acid on fathead minnow (*Pimephales promelas*) fatty acyl-CoA oxidase activity, circulating steroids, and reproduction in outdoor microcosms. *Environ Toxicol Chem* 2004;23:1912–9.
- Orrenius S, Gogvadze A, Zhivotovskiy B. Mitochondrial oxidative stress: implications for cell death. *Annu Rev Pharmacol* 2007;47:143–83.
- Pfaffl MW. A new mathematical model for relative quantification in real-time RT-PCR. *Nucleic Acids Res* 2001;29:2002–7.
- Renner R. Growing concern over perfluorinated chemicals. *Environ Sci Technol* 2001;35:154A–60A.
- Seacat AM, Thomford PJ, Hansen KJ, Clemen LA, Eldridge SR, Elcombe CR, et al. Sub-chronic dietary toxicity of potassium perfluorooctanesulfonate in rats. *Toxicology* 2003;183:117–31.
- Shearer BG, Hoekstra WJ. Recent advances in peroxisome proliferator-activated receptor science. *Curr Med Chem* 2003;10:267–80.
- Shi XJ, Yeung LWY, Lam PKS, Wu RSS, Zhou BS. Protein profiles in zebrafish (*Danio rerio*) embryos exposed to perfluorooctane sulfonate. *Toxicol Sci* 2009;110:334–40.
- Smithwick M, Muir DC, Mabury SA, Solomon KR, Martin JW, Sonne C, et al. Perfluoroalkyl contaminants in liver tissue from East Greenland polar bears (*Ursus maritimus*). *Environ Toxicol Chem* 2005;24:981–6.
- So MK, Yamashita N, Taniyasu S, Jiang QJ, Giesy JP, Chen K, et al. Health risks in infants associated with exposure to perfluorinated compounds in human breast milk from Zhoushan, China. *Environ Sci Technol* 2006;40:2924–9.
- Song W, Zou ZY, Xu F, Gu XX, Xu XF, Zhao QS. Molecular cloning and expression of a second zebrafish aldehyde dehydrogenase 2 gene (aldh2b). *DNA Seq* 2006;17:262–9.
- Takacs ML, Abbott BD. Activation of mouse and human peroxisome proliferator-activated receptors (alpha, beta/delta, gamma) by perfluorooctanoic acid and perfluorooctane sulfonate. *Toxicol Sci* 2007;95:108–17.
- Tao L, Kannan K, Wong CM, Arcaro KF, Butenhoff JL. Perfluorinated compounds in human milk from Massachusetts, USA. *Environ Sci Technol* 2008;42:3096–101.
- Vanden Heuvel JP, Thompson JT, Frame SR, Gillies PJ. Differential activation of nuclear receptors by perfluorinated fatty acid analogs and natural fatty acids: a comparison of human, mouse, and rat peroxisome proliferator-activated receptor-alpha, -beta, and -gamma, liver X receptor-beta, and retinoid X receptor-alpha. *Toxicol Sci* 2006;92:89–476.
- Voso MT, Hohaus S, Guidi F, Fabiani E, D'Alo F, Groner S, et al. Prognostic role of glutathione S-transferase polymorphisms in acute myeloid leukemia. *Leukemia* 2008;22:1685–91.
- Wei Y, Chan LL, Wang D, Zhang H, Wang J, Dai J. Proteomic analysis of hepatic protein profiles in rare minnow (*Gobiocypris rarus*) exposed to perfluorooctanoic acid. *J Proteome Res* 2008;7:1729–39.
- Wetmore BA, Merrick BA. Toxicoproteomics: proteomics applied to toxicology and pathology. *Toxicol Pathol* 2004;32:619–42.
- Wilkinson KD, Tashayev VL, Oconnor LB, Larsen CN, Kasperek E, Pickart CM. Metabolism of the polyubiquitin degradation signal: structure, mechanism, and role of isopeptidase-T. *Biochem Us* 1995;34:14535–46.
- Yang Q, Xie Y, Eriksson AM, Nelson BD, DePierre JW. Further evidence for the involvement of inhibition of cell proliferation and development in thymic and

- splenic atrophy induced by the peroxisome proliferator perfluorooctanoic acid in mice. *Biochem Pharmacol* 2001;62:1133–40.
- Youssef J, Badr M. Extraperoxisomal targets of peroxisome proliferators: mitochondrial, microsomal, and cytosolic effects. Implications for health and disease. *Crit Rev Toxicol* 1998;28:1–33.
- Zamzami N, Larochette N, Kroemer G. Mitochondrial permeability transition in apoptosis and necrosis. *Cell Death Differ* 2005;12:1478–80.
- Zhang HX, Shi ZM, Liu Y, Wei YH, Dai JY. Lipid homeostasis and oxidative stress in the liver of male rats exposed to perfluorododecanoic acid. *Toxicol Appl Pharmacol* 2008;227:16–25.